2015 International Conference on Unmanned Aircraft Systems (ICUAS)
Denver Marriott Tech Center
Denver, Colorado, USA, June 9-12, 2015

Autonomous search and tracking of objects using model predictive control of unmanned aerial vehicle and gimbal: Hardware-in-the-loop simulation of payload and avionics*

Espen Skjong[1], Stian Aas Nundal[2], Frederik Stendahl Leira[3] and Tor Arne Johansen[4]

Abstract— **This paper describes the design of model predictive control (MPC) for an unmanned aerial vehicle (UAV) used to track objects of interest identified by a real-time camera vision (CV) module in a search and track (SAT) autonomous system. A fully functional UAV payload is introduced, which includes an infra-red (IR) camera installed in a two-axis gimbal system. Hardware-in-loop (HIL) simulations are performed to test the MPC's performance in the SAT system, where the gimbal attitude and the UAV's flight trajectory are optimized to place the object to be tracked in the center of the IR camera's image.**

I. Introduction

The recent up-spring of commercial availability of small unmanned aerial vehicles (UAV) has lead to their use in many different applications involving inspections of structures, surveillance, and tracking of objects in less accessible environments. A lot of research has been carried out to extend the UAV's area of application, especially in areas where UAVs can increase safety. This includes search and rescue (SAR) applications, where UAVs equipped with cameras are used to map large areas and find missing objects and persons.

[1] describes a SAR system using a fixed wing UAV equipped with a camera sensor. By searching a predefined area, likelihood functions are made to determine the likelihood of localizing the object at a given location. The likelihood functions are merged into a larger mapping, a probability density function (PDF), which is maintained to express the most likely location of the target. The UAV's and the camera sensor's paths are generated from the PDF to maximize the likelihood of detecting the object of interest. The main possible limitations of this approach is that it may not easily extend to an arbitrary number of objects, and that localizing a moving target would greatly complicate the process.

[2] describes the combination of decentralized MPC (DMPC) and mixed-integer linear programming (MILP) used for collision avoidance and UAV path planning. [3] uses similar techniques for search planning. [4] use the UAV's kinematics together with low level avionics to design a non-linear MPC controlling a fixed wing UAV. Their MPC is designed to track a pre-planned flight path based on error dynamics. Even though MPC has proved to be an effective control approach in UAV path planning, the MPCs designed by [2] and [4] does not include gimbal control and on-line flight trajectory generation.

Analogue to UAV SAR systems, search and track (SAT) systems using UAVs have also been a hot topic of research. [5] describes an ice management SAT system using an UAV equipped with sensors such as IR camera, laser and different microwave technologies. [6] describes the control of flight paths of multiple UAVs where the goal is to steer the UAV's in predefined trajectories avoiding collisions. Such a system could be advantageous when searching large areas and tracking multiple objects of interest. The fleet of UAVs could easily increase the area to be searched if used in a SAT system, thus increase the efficiency of the system tracking multiple objects at once. [7] consider task allocation and path planning for multiple UAVs using MILP.

In this paper, the focus is on the development and implementation of a novel search and track

*Centre for Autonomous Marine Operations and Systems (AMOS), Department of Engineering Cybernetics, Norwegian University of Science and Technology
[1]e-mail: espen.skjong@itk.ntnu.no
[2]e-mail: s.nundal@gmail.com
[2]e-mail: frederik.leira@itk.ntnu.no
[2]e-mail: tor.arne.johansen@itk.ntnu.no

(SAT) payload system using a MPC, which includes the design of the controller responsible for steering the UAV towards regions of interest and optimal gimbal attitude placing objects of interest in the center of the camera image. In particular we develop a SAT system where we assume a computer vision (CV) module [8], [9] is working directly with the UAV autopilot and the MPC in an autonomous decision making process. This allows the system to simultaneously detect and track multiple moving objects in an efficient manner. Placing the control of the UAV's flight and the gimbal's attitude trajectories in the same controller would enable system flexibility, which could be proven advantageous when the quality of the object tracking is to be increased. The main contributions of this paper are in the formulation and implementation of the MPC generating both the UAV and gimbal trajectories as well as system integration and HIL testing of avionics, payload and operator station.

The remainder of the paper is organized as follows. First, the overall UAV payload and system are described. This includes a short description of each independent module and their respective tasks. Second, an in-depth description of the MPC used to develop and implement a SAT system onboard an UAV is given. Third, hardware-in-the-loop (HIL) tests are described, and the system's performance is evaluated. Finally the paper is summarized with a brief conclusion.

II. System Topology

The object tracking system consists of several components and subsystems. Figure 1 describes the information flow between the main system components. The object tracking system includes an autopilot (flight control), a CV module, an object handler, and a MPC module. The CV module is responsible for identifying objects of interest using an infra-red (IR) camera, and estimates object positions and velocities. The estimated object information is sent to the object handler which selects the object(s) to be tracked based on UAV and object positions and attitudes. The MPC module, based on the UAV's attitude, position and velocity, calculates an optimal flight trajectory and optimal gimbal attitude to place the object(s) to be tracked within the camera's image.

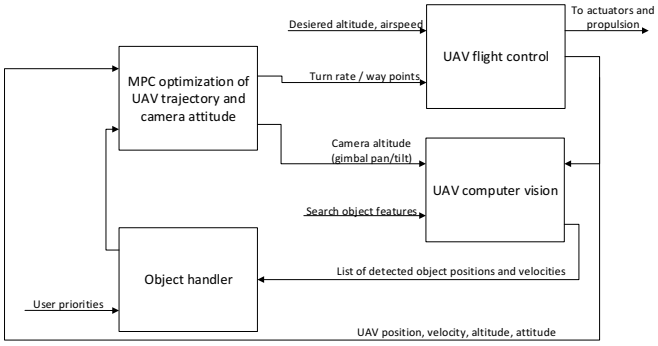

Fig. 1: Overall object tracking system description.

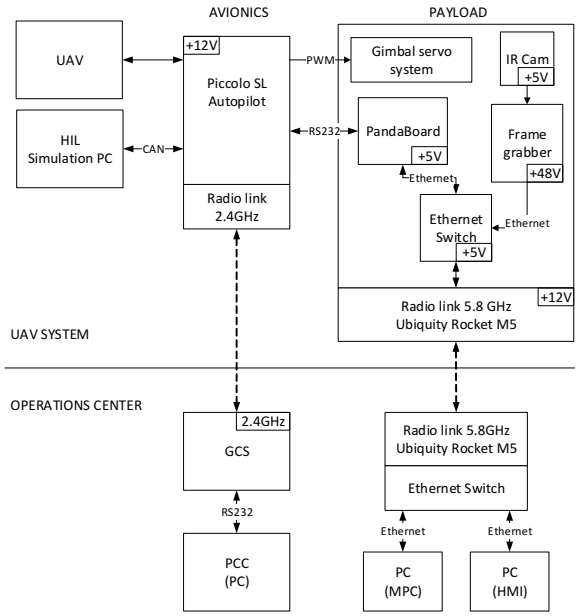

Fig. 2: Total system integration for HIL simulations.

A dedicated computational device, the CV module, an IR camera and radio links are all part of the UAV's payload. Multiple radio links are installed in the UAV's payload enabling remote control of the object tracking system from a remote control station, known as the ground control station (GCS), where also the MPC is run on a dedicated computer. A local Ethernet connects the on-board computer with the IR camera (through a frame grabber) and one of the radio links. The autopilot and the onboard computer is directly connected by a serial interface where telemetry data is available to the onboard computer and commands can be received by the autopilot. The ground station includes radio links, an object tracking HMI (Human-Machine-

Interface) and a remote autopilot control software solution. The flight operator managing the command center is able to switch between manual, automatic and autonomous flight modes, where the latter represents the object tracking system when the MPC controls the UAV's path and the gimbal's attitude. Figure 2 presents the total system integration for HIL simulations, see section IV for more details.

The UAV search and track system includes two modes, i) *search* and ii) *track*. The search mode is used to find objects to track within a predefined area. The operator defines the search area which is used by the UAV system to make a search grid and gimbal swipe motion which would cover the whole predefined area [10], [3], [11]. When the search grid is partly covered and objects are found, the operator could switch the system mode to *track*, which enables object tracking. In this paper we will focus on the *track* mode of the total UAV system.

III. Model Predictive Control

A dedicated autopilot is used to control the UAV's flight, and uses way points as control inputs. The gimbal system is controlled by reference angles for tilt (α) and pan (β). Hence, the control objective would be to calculate optimal trajectories for the UAV's flight and the gimbal's attitude to place the object(s) of interest in the camera image. The control approach is a MPC module feeding both the UAV and the gimbal system with optimal control inputs. When designing the MPC the following is assumed:

Assumption 1: *The CV module, which is based on [8], [9], provides an object list with object positions and velocities. The object handler selects a geographically referenced object or a cluster of objects from the object list to track within a finite time horizon. The objects to be tracked at a given time horizon are selected based on the UAV's and the objects' positions and headings, as well as the objects' priorities.*

Assumption 2: *The autopilot controls the UAV relative to the MPC's optimal trajectory calculations. The autopilot is also responsible for maintaining a desired air speed.*

A. UAV and object kinematics

The UAV measurements and the estimated object states from the CV module are referenced to different frames, hence two different coordinate frames are defined, a local body frame fixed to the UAV $\{\mathrm{u}\}$ and an ENU frame fixed to the earth $\{\mathrm{e}\}$. In addition, a third reference frame $\{\mathrm{g}\}$ with origin in the center of the gimbal can be defined. Figure 3 summarizes the coordinate frames. In the object

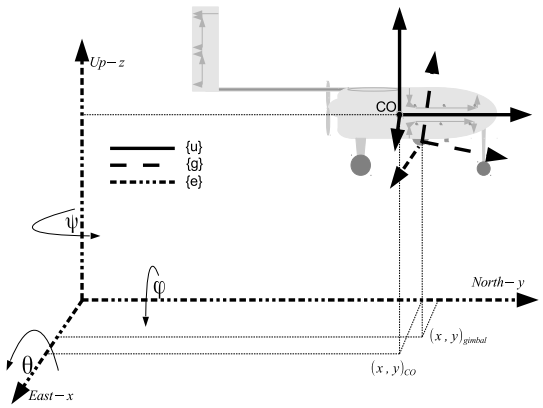

Fig. 3: Representation of the ENU, body and gimbal frames.

tracking system only horizontal plane motion is considered. This is because the altitude is assumed constant and the roll and pitch angles are compensated for by the gimbal. By these assumptions the position and heading can be expressed in frame $\{\mathrm{e}\}$ by

$$\boldsymbol{\eta} = \begin{bmatrix} x, & y, & \psi \end{bmatrix}^\top. \tag{1}$$

x and y are north and east positions, respectively, relative a chosen origin, and ψ is the yaw angle. This forms a 3DOF system where the associated velocities are given in frame $\{\mathrm{u}\}$ by

$$\boldsymbol{\nu} = \begin{bmatrix} \nu_x^u, & \nu_y^u, & r \end{bmatrix}^\top. \tag{2}$$

Hence, the translations, rotations and their derivatives are now related by

$$\dot{\boldsymbol{\eta}} = \mathbf{R}_z(\psi)\boldsymbol{\nu}. \tag{3}$$

To assume no wind disturbances is a poor assessment. Since wind disturbances would almost always be present and introduce a crab angle σ,

the UAV's course χ can be stated as the sum of the crab σ and the yaw angle ψ, i.e. [12]

$$\chi = \psi + \sigma, \tag{4}$$

where the crab angle is given by

$$\sigma = \arctan\left(\frac{\nu_y^u}{\nu_x^u}\right). \tag{5}$$

Hence, using the course angle χ and course rate r_χ eq. (3) can be rewritten as

$$\dot{\tilde{\boldsymbol{\eta}}} = \mathbf{R}_z(\chi)\tilde{\boldsymbol{\nu}}, \tag{6}$$

where $\tilde{\boldsymbol{\eta}} = [x, y, \chi]^\top$ and $\tilde{\boldsymbol{\nu}} = [\nu^a, 0, r_\chi]^\top$ where $\nu^a = \sqrt{\left(\nu_x^u\right)^2 + \left(\nu_y^u\right)^2}$. Table I summarizes the notation.

TABLE I: Symbols and notation.

Symbol	Explanation	Unit
$\mathbf{r} = [x, y, z]^\top$	UAV's position vector in frame {e}	m
$\boldsymbol{\eta} = [x, y, \psi]^\top$	UAV's position and attitude vector relative frame {e}	m rad
$\boldsymbol{\nu} = [\nu_x^u, \nu_y^u, r]^\top$	UAV's velocity and angular rate vector in frame {u} relative {e}	$\frac{m}{s}$ $\frac{rad}{s}$
χ	UAV's course angle relative frame {e}	rad
r_χ	UAV's course rate relative frame {e}	$\frac{rad}{s}$
$\boldsymbol{\Theta} = [\phi, \theta, \psi]^\top$	UAV's roll, pitch and yaw angles relative frame {e}	rad
$\dot{\boldsymbol{\Theta}} = [p, q, r]^\top$	UAV's roll, pitch and yaw rates relative frame {e}	$\frac{rad}{s}$
$\mathbf{r}_j^{obj} = \left[x_j^{obj}, y_j^{obj}, z_j^{obj}\right]^\top$	Object j's position vector in frame {e}	m
$\boldsymbol{\nu}_j^{obj} = \left[\nu_{x,j}^{obj}, \nu_{y,j}^{obj}, \nu_{z,j}^{obj}\right]^\top$	Object j's velocity vector in frame {e}	$\frac{m}{s}$
$[\alpha, \beta]$	Gimbal's tilt and pan angle relative frame {u}	rad

B. Gimbal kinematics

The gimbal system should be given optimal control inputs, i.e. optimal tilt (α) and pan (β) angles relative the frame $\{\mathrm{u}\}$. For each object, gimbal attitude can be calculated, placing each object of interest in the middle of the camera image. Given an object j with position $\mathbf{r}_j^{obj} = \left[x_j^{obj}, y_j^{obj}, z_j^{obj}\right]^\top$ in the frame $\{\mathrm{e}\}$ and the position of the center of the camera's image plane relative to frame $\{\mathrm{e}\}$, $\mathbf{r}^c = [x^c, y^c, z^c]^\top$ the desired tilt and pan angles placing object j in the middle of the camera image can be stated in the form

$$\begin{aligned} \alpha_{d,j} &= \lambda\left(\mathbf{r}^c, \mathbf{r}_j^{obj}, \phi, \theta, \chi\right) \\ \beta_{d,j} &= \mu\left(\mathbf{r}^c, \mathbf{r}_j^{obj}, \phi, \theta, \chi\right). \end{aligned} \tag{7}$$

The desired gimbal attitude expressed in eq. (7) uses the UAV's attitude to rotate the object coordinates to level the UAV. This can be seen as rotating the earth frame about the UAV's center of origin opposite to the UAV's attitude, and use the new coordinates to calculate the desired gimbal attitude relative each object of interest. The rotation of the object coordinates is illustrated in figure 4, and can for object j be stated as

$$\begin{aligned} \hat{\mathbf{r}}_j^{obj} = \mathbf{r} + \\ \mathbf{R}_z(\psi)\mathbf{R}_y(-\phi)\mathbf{R}_x(-\theta)\mathbf{R}_z^\top(\psi)\left(\mathbf{r}_j^{obj} - \mathbf{r}\right). \end{aligned} \tag{8}$$

Using the resulting coordinates, eq. (8), the desired gimbal attitude can be calculated by simple trigonometric considerations. Before proceeding with the calculations of α_d and β_d the orientation of the gimbal attitude has to be defined.

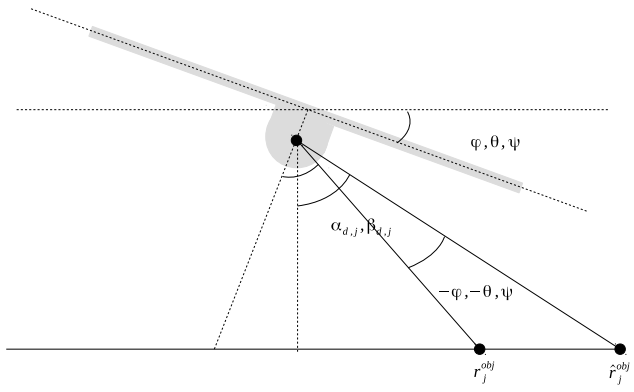

Fig. 4: Rotating object j coordinates to counteract the UAV's attitude.

The gimbal's tilt angle is bounded within $\alpha \in [\alpha_{min}, \alpha_{max}]$, where $\alpha = 0$ is defined when the camera is pointing down perpendicular to the

earth's surface assuming a leveled flight ($\phi = \theta = 0$), and $\alpha = \frac{\pi}{2}$ when the camera is pointing parallel to the horizontal plane given by the x and y axes in frame $\{\mathrm{u}\}$. The gimbal's pan angle is bounded within $\beta \in [\beta_{min}, \beta_{max}]$, where $\beta = 0$ is defined when the camera is pointing towards the UAV's nose, assuming zero tilt angle, and $\beta = \pi$ when the camera is pointing towards the UAV's back. The positive direction of rotation is counter-clockwise.

It can be shown that the desired gimbal attitude for object j can be stated as [13]

$$\alpha_{d,j} = \arctan\left(\frac{\sqrt{(x^c - \hat{x}_j^{obj})^2 + (y^c - \hat{y}_j^{obj})^2}}{z^c - \hat{z}_j^{obj}}\right), \tag{9}$$

$$\beta_{d,j} = \begin{cases} -\arctan\left(\frac{\hat{x}_j^{obj} - x_c}{\hat{y}_j^{obj} - y_c}\right) - \psi & \forall x_c \leq \hat{x}_j^{obj} \wedge y_c < \hat{y}_j^{obj} \\ -\pi + \arctan\left(\frac{\hat{x}_j^{obj} - x_c}{y_c - \hat{y}_j^{obj}}\right) - \psi & \forall x_c \leq \hat{x}_j^{obj} \wedge y_c > \hat{y}_j^{obj} \\ \pi - \arctan\left(\frac{x_c - \hat{x}_j^{obj}}{y_c - \hat{y}_j^{obj}}\right) - \psi & \forall x_c \geq \hat{x}_j^{obj} \wedge y_c > \hat{y}_j^{obj} \\ \arctan\left(\frac{x_c - \hat{x}_j^{obj}}{\hat{y}_j^{obj} - y_c}\right) - \psi & \forall x_c \geq \hat{x}_j^{obj} \wedge y_c < \hat{y}_j^{obj} \\ -\frac{\pi}{2} & \forall x_c < \hat{x}_j^{obj} \wedge y_c = \hat{y}_j^{obj} \\ \frac{\pi}{2} & \forall x_c > \hat{x}_j^{obj} \wedge y_c = \hat{y}_j^{obj} \end{cases}. \tag{10}$$

C. Object dynamics

The objects' positions and velocities relative frame $\{\mathrm{e}\}$ are provided by the CV module and used by the MPC module to predict object positions throughout the MPC horizon, i.e.

$$\begin{aligned} x_{j,t+T}^{obj} &= x_{j,t}^{obj} + \sum_{k=t+1}^{t+T} \nu_{x,j,t}^{obj} \Delta_k \\ y_{j,t+T}^{obj} &= y_{j,t}^{obj} + \sum_{k=t+1}^{t+T} \nu_{y,j,t}^{obj} \Delta_k, \end{aligned} \tag{11}$$

with the MPC horizon $[t, t+T]$. As can be seen from the last term in eq. 11, the future object velocity is assumed constant and equal to the instantaneous velocity, i.e. $\nu_{j,k}^{obj} = \nu_{j,t}^{obj} \quad \forall k \in [t, t+T]$.

D. Cost function

The control problem, where the objective is to use the information from each object identified by the CV module, to calculate optimal UAV and gimbal controls based on the UAV's and the gimbal's attitude, can be formulated as a Lagrange problem with integral quadratic cost given by

$$\begin{aligned} J_{t+T} =& \frac{1}{2} \sum_{i=t}^{t+T} \left[(\mathbf{h}(\mathbf{z}_i) - \mathbf{h}_d)^\top \mathbf{Q} (\mathbf{h}(\mathbf{z}_i) - \mathbf{h}_d) \right] \\ &+ \frac{1}{2} \sum_{i=t}^{t+T} \left[\mathbf{u}_i^\top \mathbf{R} \mathbf{u}_i \right], \end{aligned} \tag{12}$$

where the state vector $\mathbf{z}_k$ is given by

$$\mathbf{z}_k = \left[x_k, y_k, \chi_k, \alpha_k, \beta_k, x_{1,k}^{obj}, y_{1,k}^{obj}, \ldots, x_{n,k}^{obj}, y_{n,k}^{obj} \right]^\top, \tag{13}$$

and n is given by the length of the object list.

The matrices $\mathbf{Q} \in \mathbb{R}^{3n \times 3n}$ and $\mathbf{R} \in \mathbb{R}^{3 \times 3}$ are diagonal weight matrices. The controlled variables, $\mathbf{u}$ at time step k are given by

$$\mathbf{u}_k = \left[\dot{\alpha}_k, \dot{\beta}_k, r_{\chi,k} \right]^\top. \tag{14}$$

The distance between the UAV and the objects of interest, together with the measured gimbal attitude, are given by the $\mathbb{R}^{3n \times 1}$ mapping

$$\mathbf{h}(\mathbf{z}_k) = \begin{bmatrix} \sqrt{(x_{1,k} - x_{1,k}^{obj})^2 + (y_{1,k} - y_{1,k}^{obj})^2} \\ \vdots \\ \sqrt{(x_{n,k} - x_{n,k}^{obj})^2 + (y_{n,k} - y_{n,k}^{obj})^2} \\ \alpha_k \\ \beta_k \\ \vdots \\ \alpha_k \\ \beta_k \end{bmatrix}. \tag{15}$$

The desired distance between the UAV and the objects, together with the desired gimbal attitude for each object, are given by

$$\mathbf{h}_d = \left[\delta \mathbf{1}^{n \times 1}, \alpha_{d,1,k}, \beta_{d,1,k}, \ldots, \alpha_{d,n,k}, \beta_{d,n,k} \right]^\top, \tag{16}$$

where δ equals the UAV's desired turning radius. This leads to the UAV loitering above the objects with a given radius. Instead of using α_k and β_k as controls, the rates $\dot{\alpha}_k$ and $\dot{\beta}_k$ are used. This adds constraints and penalties for the gimbal's angular rates as well as the UAV's course rate in the last term of eq. (12), which is added to prevent rapid changes in the gimbal's attitude and the UAV's course.

E. Constraints

The UAV's physical limitations are tied to its maneuverability. The autopilot maintains the UAV's speed and altitude, and also keeps the UAV levelled. The autopilot is also compensating for wind gusts and environmental disturbances. Hence, only the turn radius, which is dependent on the course rate r_χ, will have impact on the calculation of the trajectory. Assuming the course rate is bounded, i.e. $r_{k,\chi} \in [r_{\chi,min}, r_{\chi,max}]$, and the UAV's cruising speed is given by ν_c, the minimum turning radius δ_{min} can be calculated as

$$\delta_{min} = \frac{\nu_c}{max\left(r_{\chi,min}, r_{\chi,max}\right)}, \tag{17}$$

which means δ should be designed according to

$$\delta \geq \frac{\nu_c}{max\left(r_{\chi,min}, r_{\chi,max}\right)}. \tag{18}$$

One should note that if δ is too large, the gimbal's tilt angle would be saturated when trying to place the object j in the camera image. If δ is too small, the UAV's manoeuvre would be impaired due to infeasible trajectories, which in turn could lead to a low quality of the object tracking.

As mentioned earlier, the gimbal's attitude is bounded relative the gimbal's physical or operational limitations, i.e. $\dot{\alpha}_k \in [\dot{\alpha}_{min}, \dot{\alpha}_{max}]$ and $\dot{\beta}_k \in \left[\dot{\beta}_{min}, \dot{\beta}_{max}\right]$. To compensate for turbulence, it may be a necessity with fast response. To summarize, the constraints are given as

$$r_{\chi,min} \leq r_{\chi,k} \leq r_{\chi,max}, \quad \frac{rad}{s} \tag{19}$$

$$\alpha_{min} \leq \alpha_{d,j,k} \leq \alpha_{max}, \quad rad \tag{20}$$

$$\beta_{min} \leq \beta_{d,j,k} \leq \beta_{max}, \quad rad \tag{21}$$

$$\dot{\alpha}_{min} \leq \dot{\alpha}_k \leq \dot{\alpha}_{max}, \quad \frac{rad}{s} \tag{22}$$

$$\dot{\beta}_{min} \leq \dot{\beta}_k \leq \dot{\beta}_{max}, \quad \frac{rad}{s}. \tag{23}$$

F. Implementation

The *ACADO toolkit*[1] [14] is used to implement the MPC formulation using the ACADO C++ API with the Gauss-Newton Hessian approximation. The MPC formulation must be rewritten using slack variables to prevent the problem becoming infeasible [15]. The MPC problem formulation does not include any disturbance models, e.q. wind models, due to closed loop feedback provided within the autopilot. New UAV and gimbal measurements for the initialization of each MPC horizon provides the necessary trajectory corrections. The MPC interfaces the autopilot using an API protocol over serial connection. After each MPC calculation, the optimal UAV and gimbal trajectories are modified by removing all elements which were impaired by the MPC's time delay while calculating the present horizon, and the first remaining optimal way-point and the gimbal attitude in the discretized trajectories are sent to the autopilot as control action.

IV. System Integration

Some of the main components used in the system are briefly addressed in this section before introducing the payload and the HIL configuration.

A. UAV and Avionics

The UAV used is the *Penguin B* from *UAV Factory*[2], while the autopilot used in the UAV system is the *Piccolo SL* from *Cloud Cap Technology*[3]. The *Piccolo Command Center* (PCC) provides remote control of the autopilot from the GCS. The DUNE library[4] provides the interface to the Piccolo autopilot through a high-level IMC protocol. A dedicated 2.4GHz radio link enables connection from the autopilot to the PCC, cf. figure 2 for a detailed description of the system integration.

B. Payload

The UAV's additional payload consists of an IR camera (*Flir Tau 2*) installed in a two-axis gimbal system (*BTC-88*[5]) and connected to an *AXIS* frame grabber, PoE (Power over Ethernet) converters, a PandaBoard[6], a radio link (*Rocket M5)* provided by *Ubiquiti Networks*[7] and a switch. The onboard generator provides a +12V power supply, and since some of the components in the payload operate with +5V and +48V, a step-down converter (12-5V

[1] www.acadotoolkit.org

[2] www.uavfactory.com

[3] www.cloudcaptech.com

[4] http://lsts.fe.up.pt/software/dune

[5] www.microuav.com

[6] www.pandaboard.org

[7] www.ubnt.com

DC/DC) and a step-up converter (12-48V DC/DC) are installed in the UAV's payload. The payload is presented in figure 5.

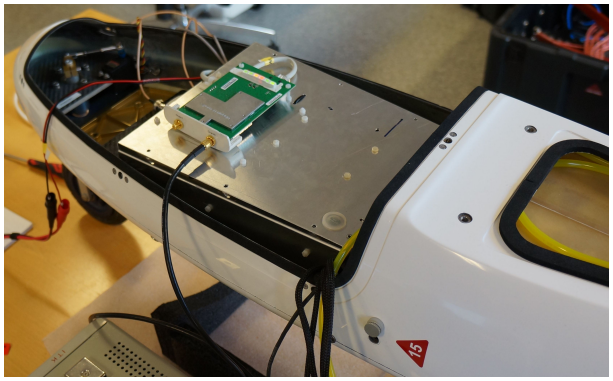

Fig. 5: The UAV's payload shielded in an aluminum housing. The 5.8GHz radio link is mounted on the top of the housing.

C. HIL Configuration

In this section the CV module is disregarded and the object list are simulated. Figure 2 presents the system integration and the different interfaces which is used in the HIL simulations. A CAN interface connects a simulator with the autopilot. The simulator (*FlightGear*) simulates the UAV's motions and includes disturbance models such as wind gusts and turbulence. The PCC is connected with Piccolo via the GCS, which communicates with the onboard Piccolo through a 2.4GHz radio link. The onboard Piccolo is connected to the PandaBoard with a serial (RS232) interface. In this HIL configuration, the MPC is running on a computer in the ground operation center. The MPC and an in-house object tracking HMI communicates with the PandaBoard over a 5.8GHz radio link. The 5.8GHz radio link is dedicated for payload use to avoid interference with the 2.4GHz link between the autopilot and the PCC. As can be seen in figure 2, the MPC communicates with the autopilot through the PandaBoard in the payload. For more information regarding the system integration and the payload design we refer to [13].

V. Results

Using the HIL configuration described in the previous section four object tracking scenarios are simulated. The first scenario is based on four stationary objects which forms a square with sides of 2000 meters with center in the $\{e\}$ frame's origin. The second scenario uses the same object configuration as in the first scenario, but the objects are moving away from each other, parallel to the square's diagonals. The third scenario is constructed using three objects placed in equilateral triangular configuration with sides of 2000 meters, where the objects are moving towards each other. In all scenarios the MPC horizon is set to be short. This is due to heavy computational costs as an on-line[8] MPC with a long horizon impairs the system's real-time properties. The altitude is fixed to 100 meters in all test cases. Before discussing each scenario, the structure of the resulting figures 6-10 is addressed.

The large plot to the left represents a north-east (NE) plot of the UAV's flight path. The black circle represents the UAV and the blue frame is the projected camera image frame down on earth, calculated by assuming a pinhole camera model [13]. The blue cross located within the projected camera image represents the camera image's center. The objects are marked in the plot by coloured circles, red indicating an untracked object, blue indicating an object which is being tracked and green indicating a previously tracked object. The small plots to the right in each figure represents some of the UAV's and the gimbal's dynamics within the time frame from the last calculated MPC horizon. From top, left to right: ψ, α and β. From bottom, left to right: r, $\dot{\alpha}$ and $\dot{\beta}$.

A. Four stationary objects

In this scenario the MPC horizon is set to 5 seconds. Figure 6 shows the UAV has entered a circular motion around the third object to be tracked, after finishing the tracking of the first two objects. This means the object handler has given the object information for the third object to the MPC. As can be seen, the UAV's circular motion enables nearly constant gimbal attitude, in which provides a good image quality. It can also be seen that the UAV's trajectory between the objects are straight lines which is the shortest distance between the objects.

[8]The MPC is computing new control action approximately every 2. second.

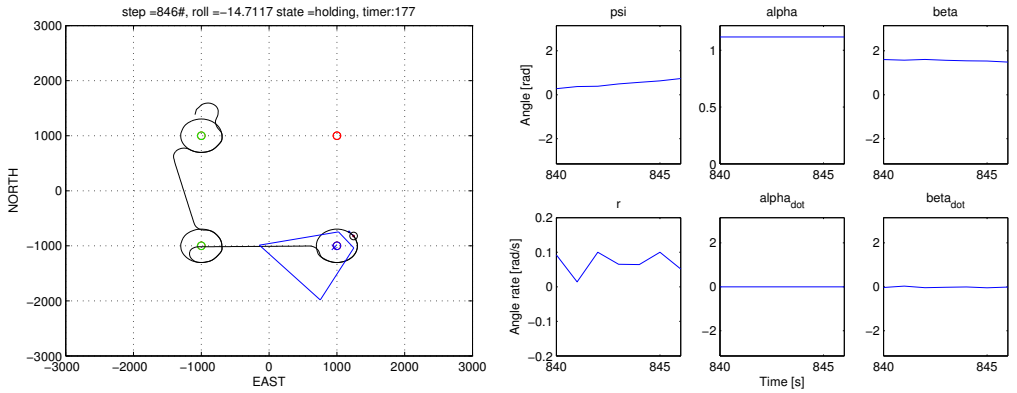

Fig. 6: Scenario 1: The UAV has entered a circular motion while tracking the third object.

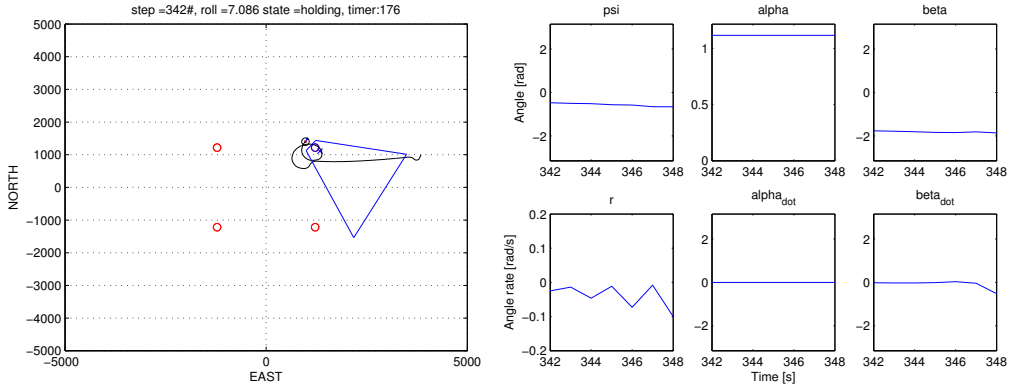

Fig. 7: Scenario 2: The UAV performing a spiral motion while tracking the first object.

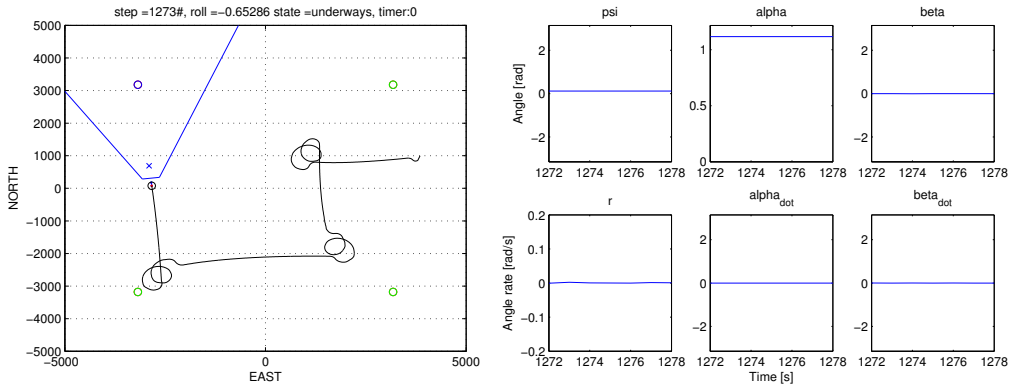

Fig. 8: Scenario 2: The UAV is headed for the fourth object to be tracked.

B. Four moving objects

In this scenario the MPC horizon is set to 6 seconds. Figure 7 shows the UAV performing a spiral motion while tracking the first object, which was given by the object handler to the MPC. The spiral motion is a result of combining optimal control of the gimbal's attitude and the UAV's flight trajectory to minimize the projected camera image's center drifting away from the object to be tracked. As can be seen, the UAV's start position is located a distance from the objects to be tracked. This is to show the UAV's path corrections due to the moving objects and the short MPC horizon. The slowly varying gimbal attitude, which is nearly constant, should provide a good tracking quality placing the objects of interest in the camera im-

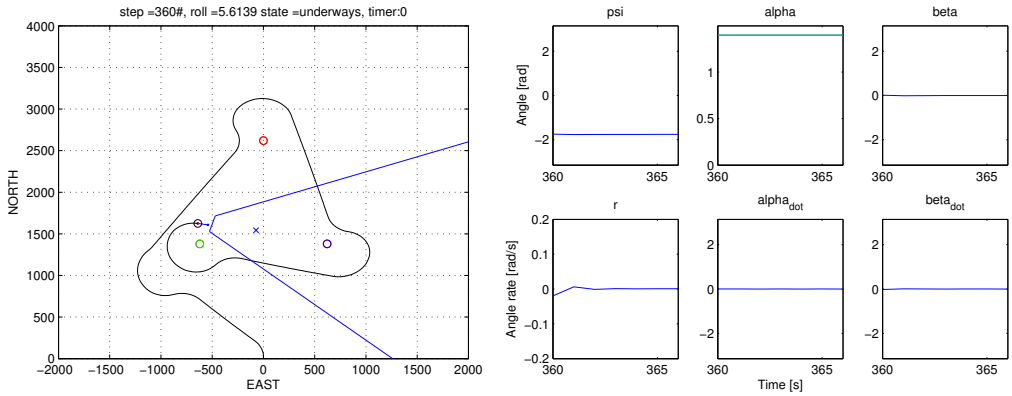

Fig. 9: Scenario 4: The UAV is tracking tree objects separately.

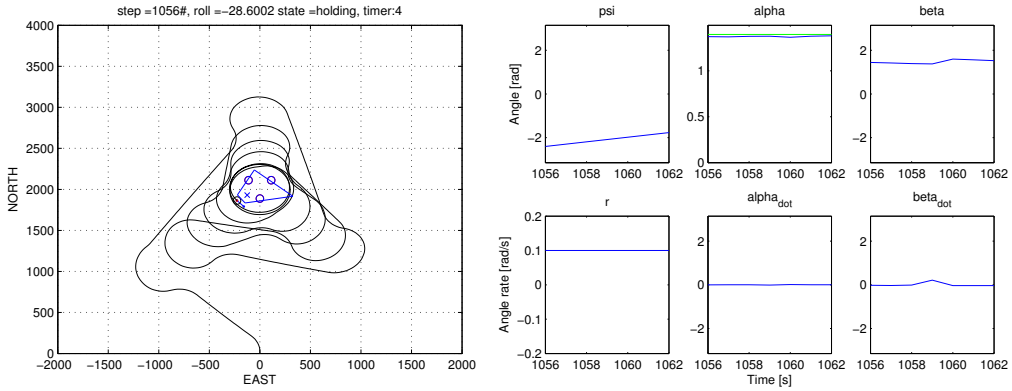

Fig. 10: Scenario 4: The UAV is tracking three objects simultaneously.

age's center.

Figure 8 shows the UAV has finished tracking the first three objects and is currently on its way towards the forth object to be tracked. As can be seen, the UAV has tracked the objects using a spiral motion due to the objects' movements. The spiral motions enable an approximately constant gimbal attitude placing the object(s) of interest in the center of the camera image.

C. Three objects moving towards each other

This last scenario shows the object handler grouping objects to be tracked simultaneously if the objects are close enough to each other. The MPC horizon is set to 5 seconds. Figure 9 shows that the objects have been tracked a shorter time interval than in the previous test cases. This is due to the commands from the object handler. Figure 10 shows the three objects that are close enough to be tracked simultaneously, hence all three objects were sent to the MPC by the object handler. As can be seen, all three objects are within the projected camera image while the UAV has entered a circular motion, and only small variations in the gimbal attitude are present during the horizon. This is a result of the UAV's heading rate r being approximately constant, thus the UAV has entered an optimal state while tracking the objects.

VI. Conclusion

A MPC formulation controlling the UAV's flight and the gimbal's attitude has been outlined. A fully functional UAV payload was briefly presented and described according to the configuration and system integration of the HIL simulation.

HIL simulations of the object tracking system were presented, which emphasise that MPC could be a viable camera-based autonomous control solution used in SAT missions in an embedded UAV platform. Mounting the MPC onboard the UAV would be feasible and could increase the system's operational limitations beyond LOS operations

by implementation additional safety mechanisms. However, an onboard MPC will require a more powerful computer than the PandaBoard.

By calculating control trajectories for the UAV's flight trajectory and the gimbal's attitude in the same controller, a high degree of system flexibility is introduced where the UAV and the gimbal are controlled to cooperate in the process of placing the object(s) to be tracked in the center of the camera image with minimal drifting decreasing the quality of the object tracking mission.

ACKNOWLEDGEMENT

This work has been carried out at the Centre for Autonomous Marine Operations and Systems (AMOS). The Norwegian Research Council is acknowledged as the main sponsor of AMOS. This work was supported by the Research Council of Norway through the Centres of Excellence funding scheme, Project number 223254 - AMOS.

REFERENCES

[1] R. Sengupta, J. Connors, B. Kehoe, Z. Kim, T. Kuhn, and J. Wood, "Final report - autonomous search and rescue with ScanEagle, U.C. Berkeley," September 2010.

[2] A. Richards and J. How, "Decentralized model predictive control of cooperating uavs," in *43rd IEEE Conference on Decision and Control, 2004. CDC.*, vol. 4, 2004, pp. 4286–4291 Vol.4.

[3] E. J. Forsmo, E. I. Grøtli, T. I. Fossen, and T. A. Johansen, "Optimal search mission with unmanned aerial systems using MILP," in *Proc. of the International Conference on Unmanned Aircraft Systems*, Atlanta, Georgia, USA, May 28-31 2013, pp. 253–259.

[4] Y. Kang and J. Hedrick, "Linear tracking for a fixed-wing uav using nonlinear model predictive control," *IEEE Transactions on Control Systems Technology*, vol. 17, no. 5, pp. 1202–1210, 2009.

[5] J. Haugen, L. Imsland, S. Lset, and R. Skjetne, "Ice observer system for ice management operations," in *Int. Offshore (Ocean) and Polar Eng. Conf. (ISOPE)*, vol. 21, 2011, pp. 1120–1127.

[6] E. Xargay, I. Kaminer, A. Pascoal, N. Hovakimyan, V. Dobrokhodov, V. Cichella, A. Aguiar, and R. Ghabcheloo, "Time-critical cooperative path following of multiple uavs over time-varying networks," *AIAA Journal of Guidance, Control, and Dynamics, 2013*, vol. 36, pp. 499–516, 2013.

[7] E. I. Grøtli and T. A. Johansen, "Task assignment for cooperating uavs under radio propagation path loss constraints," in *American Control Conference (ACC), 2012*, June 2012, pp. 3278–3283.

[8] F. S. Leira, K. Trnka, T. I. Fossen, and T. A. Johansen, "A ligth-weight thermal camera payload with georeferencing capabilities for small fixed-wing uavs," in *International Conference on Unmanned Aircraft Systems, Denver, 2015*.

[9] F. S. Leira, T. A. Johansen, and T. I. Fossen, "utomatic detection, classification and tracking of objects in the ocean surface from uavs using a thermal camera," in *IEEE Aerospace Conference, Big Sky, 2015*.

[10] J. George, S. P. B., and J. Sousa, "Search strategies for multiple uav search and destroy missions," *Journal of Intelligent & Robotic Systems*, vol. 61, no. 1-4, pp. 355–367, 2011.

[11] C. M. Mathisen, "Search and rescue operations using a fixed-wing uav equipped with an automatically controlled gimbal," p. 156, 2014, master Thesis, NTNU, Department of Engineering Cybernetics.

[12] W. F. Phillips, *Mechanics of flight*. Hoboken, N.J. John Wiley & Sons, 2010.

[13] E. Skjong and S. A. Nundal, "Tracking objects with fixed-wing uav using model predictive control and machine vision," p. 295, 2014, Master Thesis, NTNU, Department of Engineering Cybernetics.

[14] B. Houska, H. Ferreau, M. Vukov, and R. Quirynen, "ACADO Toolkit User's Manual," http://www.acadotoolkit.org, 2009–2013, last accessed: 2014-04-20.

[15] J. Nocedal and S. Wright, *Numerical Optimization*, ser. Springer Series in Operations Research and Financial Engineering. Springer New York, 2006.